Regular Article

Development of Gold Nanorods Conjugated with Radiolabeled Anti-human Epidermal Growth Factor Receptor 2 (HER2) Monoclonal Antibody as Single-Photon Emission Computed Tomography/Photoacoustic Dual-Imaging Probes Targeting HER2-Positive Tumors

Ning Ding,[a] Kohei Sano,*[a,b] Yoichi Shimizu,[a] Hiroyuki Watanabe,[a] Takeshi Namita,[c] Tsuyoshi Shiina,[c] Masahiro Ono,[a] and Hideo Saji[a]

[a] *Department of Patho-Functional Bioanalysis, Graduate School of Pharmaceutical Sciences, Kyoto University; 46–29 Yoshida Shimoadachi-cho, Sakyo-ku, Kyoto 606–8501, Japan:* [b] *Laboratory of Biophysical Chemistry, Kobe Pharmaceutical University; 4–19–1 Motoyama Kitamachi, Higashinada-ku, Kobe 658–8558, Japan: and* [c] *Human Health Sciences, Graduate School of Medicine, Kyoto University; Kyoto 606–8507, Japan.*
Received April 28, 2020; accepted September 8, 2020

Surgery remains one of the main treatments of cancer and both precise pre- and intraoperative diagnoses are crucial in order to guide the operation. We consider that using an identical probe for both pre- and intra-operative diagnoses would bridge the gap between surgical planning and image-guided resection. Therefore, in this study, we developed gold nanorods (AuNRs) conjugated with radiolabeled anti-human epidermal growth factor receptor 2 (HER2) monoclonal antibody, and investigated their feasibility as novel HER2-targeted dual-imaging probes for both single photon emission computed tomography (SPECT) (preoperative diagnosis) and photoacoustic (PA) imaging (intraoperative diagnosis). To achieve the purpose, AuNRs conjugated with different amount of trastuzumab (Tra) were prepared, and Tra-AuNRs were labeled with indium-111. After the evaluation of binding affinity to HER2, cell binding assay and biodistribution studies were carried out for optimization. AuNRs with moderate trastuzumab conjugation (Tra2-AuNRs) were proposed as the novel probe and demonstrated significantly higher accumulation in NCI-N87 (HER2 high-expression) tumors than in SUIT2 (low-expression) tumors 96 h post-injection along with good affinity towards HER2. Thereafter, *in vitro* PA imaging and *in vivo* SPECT imaging studies were performed. In *in vitro* PA imaging, Tra2-AuNRs-treated N87 cells exhibited significant PA signal increase than SUIT2 cells. In *in vivo* SPECT, signal increase in N87 tumors was more notable than that in SUIT2 tumors. Herein, we report that the Tra2-AuNRs enabled HER2-specific imaging, suggesting the potential as a robust HER2-targeted SPECT and PA dual-imaging probe.

Key words gold nanorod; photoacoustic imaging; indium-111; single photon emission computed tomography (SPECT); human epidermal growth factor receptor 2 (HER2)

INTRODUCTION

Cancer has long been the leading cause of death worldwide.[1)] Among various cancer therapies, surgery remains one of the main treatments for many types of solid tumors, with more than 50% of cancer patients undergoing surgery each year.[2)] In fact, the cure rate of most solid tumor types can be increased 4- to 11-fold by surgical excision.[3)] In order to remove as much tumor tissue as possible, both highly precise preoperative and intraoperative diagnoses are essential.[4,5)]

Preoperative diagnostic techniques, such as nuclear medicine, including single photon emission computed tomography (SPECT) and positron emission tomography (PET), can facilitate the identification of tumors. On the other hand, during surgeries, incomplete tumor resection remains a major challenge and occurs in as many as 20 to 60% of all operations.[2)] Intraoperative diagnoses, which are usually made by performing optical imaging, can detect small tumor lesions, locate metastases, help in tumor removal completion, and thus guide surgeons during operation by enabling real-time decisions during surgery.[6)]

In the clinical setting, different agents are generally used for preoperative and intraoperative diagnoses; these include ^{18}F-fluorodeoxyglucose (FDG) for PET and indocyanine green (ICG), commonly used for fluorescence imaging,[7–10)] for instance. However, using different agents might result in difficulties in tumor localization during surgery. The development of a single molecular-targeting probe capable of providing identical information for both pre- and intraoperative diagnoses and bridging the gap between surgical planning and image-guided resection might be the solution to this issue.

In recent years, photoacoustic (PA) imaging has emerged as a new type of biomedical diagnostic method based on the PA effect, which is the formation of ultrasound waves following light absorption in optical absorbers.[11)] The quantification of the ultrasound formed by the PA effect by using transducers enables one to obtain the PA signal.[11)] Ultrasound waves exhibit much lower tissue scattering, making it possible for PA imaging to detect information in deeper tissues than fluorescence imaging and with higher sensitivity and resolution than ultrasound imaging.[12)] Although the PA imaging is still not suitable for pre-operative whole-body screening, it is a promising intraoperative imaging method, and the development of PA imaging probes for tumor detection has been strongly desired.[13)]

Currently, various PA imaging probes, including metallic

* To whom correspondence should be addressed. e-mail: ksano@kobepharma-u.ac.jp

nanoparticles and fluorescent dyes, have been reported to aid in the diagnosis of tumors.[14–18] Among them, gold materials, especially gold nanorods (AuNRs), have attracted much attention owing to the following reasons.[19] Firstly, the strong surface plasmon resonance (SPR) absorption of AuNRs enables them to absorb more light, thus generating more PA signals. Based on the same molar concentrations, PA amplitudes of AuNRs are far higher than those of other widely used PA agents, such as fluorescent dyes or carbon-based nanomaterials.[20] Secondly, the SPR absorption of the AuNRs can be easily tuned to the near-IR (NIR) window (650–1350 nm), whose absorbance by water and hemoglobin, at minimum, enables light permeation through living bodies by adjusting the shape of AuNRs. Lastly, AuNRs have a high surface area available to act as nanocarriers, which allows easy chemical modification. These facts support AuNRs as an attractive NIR light-mediated platform for PA imaging.

In this research, human epidermal growth factor receptor 2 (HER2) was chosen as the target molecule for the diagnosis of tumors owing to its close association with a poor prognosis.[21] An anti-HER2 monoclonal antibody (trastuzumab) was chosen as a HER2-targeting moiety and conjugated to the surface of AuNRs; the compound is referred to as Tra-AuNRs. To achieve preoperative HER2 imaging, we focused on SPECT. SPECT is a nuclear medical imaging technique widely used in clinics that enables whole-body scanning. Indium-111 (^{111}In; $t_{1/2} = 2.8$ d; γ-radiation, 171, 254 keV) is one of the commonly used radioisotopes that are appropriate in SPECT imaging, and trastuzumab in Tra-AuNRs can be efficiently radiolabeled with ^{111}In by using diethylenetriaminepentaacetic acid (DTPA) as a metal chelator. There was a report that gold nanoparticles were labeled with radio-isotope (^{111}In) followed by conjugation with trastuzumab for HER2-targeted SPECT imaging, but the accumulation in the tumor was not well satisfied.[22] Considering the previous data that AuNRs could highly accumulate in the tumor compared to other gold nanoparticles (gold nanoshells),[23] we planned to develop a ^{111}In-labeled Tra-AuNRs as a novel SPECT and PA dual-imaging probe.

Herein, we prepared a ^{111}In-labeled Tra-AuNRs (^{111}In-Tra-AuNRs) series containing different amounts of trastuzumab conjugated with AuNRs. The binding affinities of Tra-AuNRs toward HER2 and *in vitro* cellular binding of Tra-AuNRs to HER2-expressing tumor cells were evaluated, which was followed by an investigation of biodistribution in HER2-positive and HER2-negative tumor-bearing mice. Finally, we performed an *in vitro* PA imaging study and an *in vivo* SPECT imaging study using ^{111}In-Tra-AuNRs that exhibited a high binding affinity to HER2 and better tumor accumulation with high background contrast.

MATERIALS AND METHODS

Synthesis of Tra-AuNRs Tra-AuNRs samples were prepared by using AuNRs (Sigma-Aldrich, St. Louis, MO, U.S.A.; or Nanopartz, Salt Lake City, UT, U.S.A.) and trastuzumab (Herceptin; Roche, Basel, Switzerland). Trastuzumab was purified by using Amicon Ultra-4 (30 kDa) centrifugal filter units (Merck Millipore, Burlington, MA, U.S.A.) for three times at $4500 \times \boldsymbol{g}$ to remove all other excipients. 1-Ethyl-3-(3-dimethylaminopropyl)-carbodiimide (EDC; TCI Chemicals, Tokyo, Japan) and *N*-hydroxysulfosuccinimide sodium salt (Sulfo-NHS, TCI Chemicals, Tokyo, Japan) were mixed at concentrations of 0.29 and 0.21 M, respectively, in 0.01 mM of 2-(*N*-morpholino)ethanesulfonic acid (MES) buffer (pH: 6.5) and added to 0.8 mg/mL of an AuNRs/water solution to activate the –COOH residues of AuNRs. After 40 min of incubation at room temperature (r.t.), spared EDC and sulfo-NHS were excluded by performing Amicon Ultra-4 (50 kDa) filtration twice at $3000 \times \boldsymbol{g}$. The purified trastuzumab was then added to activated AuNRs and incubated under the following conditions: (i) AuNRs/trastuzumab = 1 : 67 in phosphate-buffered saline (PBS) with 0.05% Tween 20 (pH: 7.4), 4 h at r.t.; (ii) AuNRs/trastuzumab = 1 : 329 in phosphate buffer with 0.05% Tween 20 (pH: 8.6), 6 h at r.t.; and (iii) AuNRs/trastuzumab = 1 : 1974 in phosphate buffer with 0.05% Tween 20 (pH: 8.6), 6 h at 37 °C. The Tra-AuNRs prepared *via* these three methods were referred to as Tra1-AuNRs, Tra2-AuNRs, and Tra3-AuNRs, respectively. After the incubation, the mixture was incubated for 1 h with polyethylene glycol amine (Nanocs Inc., New York, NY, U.S.A.) and then left at 4 °C overnight. Size-exclusion chromatography (AKTA Explorer; GE Healthcare, Chicago, IL, U.S.A.) was conducted to remove excess trastuzumab with Superdex 200 10/300 GL column (GE Healthcare) eluted with PBS containing 0.05% Tween 20 at a flow rate of 0.5 mL/min.

Characterization of Tra-AuNRs To evaluate the amounts of trastuzumab conjugated to AuNRs, the following experiments were conducted. At first, trastuzumab radiolabeled with ^{111}In was prepared. The purified trastuzumab was mixed with *p*-SCN-Bn-DTPA (Macrocyclics, Plano, TX, U.S.A.) in phosphate buffer (pH: 8.6) at a 1 : 2 (trastuzumab : *p*-SCN-Bn-DTPA) reaction ratio, and the reaction concentration of trastuzumab was found to be 2.4 mg/mL. After 6 h of incubation at 37 °C, DTPA-trastuzumab (DTPA-Tra) was purified by using Amicon Ultra-4 (30 kDa) filtration and labeled with $^{111}InCl_3$ in acetate buffer (0.1 M, pH: 6.0) at r.t., followed by reaction with AuNRs as described above. This crude sample was applied to sodium dodecyl sulfate polyacrylamide gel electrophoresis (Bullet PAGE One Precast Gel; Nacalai Tesque, Kyoto, Japan), and ^{111}In-Tra-AuNRs and ^{111}In-trastuzumab were separated. The gel was analyzed by autoradiography (FUJIFILM BAS-5000; FUJIFILM, Tokyo, Japan), and the signal intensities (SIs) of bands were quantified. After evaluating the radioactivity level of the separated regions of interest corresponding to Tra-AuNRs and free trastuzumab, the number of trastuzumab molecules conjugated to AuNRs was calculated according to the following equation; (moles of reacted trastuzumab) × (SIs of ^{111}In-Tra-AuNRs)/(SIs of ^{111}In-Tra-AuNRs + SIs of ^{111}In-trastuzumab)/(moles of AuNRs).

Synthesis of ^{111}In-Tra-AuNRs For biodistribution studies, ^{111}In-Tra-AuNRs series were synthesized as described above, followed by size-exclusion chromatography purification as mentioned above.

For the SPECT imaging study, the purified DTPA-Tra2-AuNRs were mixed with $^{111}InCl_3$ and incubated in acetate buffer (pH: 6.0) at r.t. for 60 min while gently shaking. Following incubation, excess ethylenediaminetetraacetic acid (EDTA) (nEDTA/nDTPA = 10000 : 1) was added to the mixture and incubated at r.t. for 10 min. The mixture was purified by using a PD-10 column (GE Healthcare) and concentrated by using Amicon Ultra-4 (50 kDa) filtration at $2150 \times \boldsymbol{g}$ twice. The final purification was performed by using size-exclusion

chromatography (AKTA Explorer) as mentioned above. The radiochemical purity was determined by SDS electrophoresis as mentioned above. ^{111}In-DTPA-Tra1 or Tra3-AuNRs were also synthesized by reacting DTPA-Tra-AuNRs with $^{111}InCl_3$.

Stability of ^{111}In-Tra-AuNRs DTPA-Tra1-, Tra2-, or Tra3-AuNRs were synthesized and labeled with ^{111}In as described above. Probes were dissolved in PBS or mouse serum and incubated at 37 °C. To examine the stability of ^{111}In-DTPA-Tra-AuNRs after 48, 72, and 96 h of incubation, probes were loaded onto a size-exclusion column (PD-10 column) and eluted with 15 mL of PBS. The radioactivity of each fraction (1 mL) was measured, and the radiochemical purity was calculated.

Cell Culture NCI-N87 human gastric cancer cells (N87) (DS Pharma Biomedical, Osaka, Japan) (HER2-expressing cells) and human pancreatic cancer cells (SUIT-2; Japanese Collection of Research Bioresources Cell Bank, Osaka, Japan) (HER2-low-expressing cells) were maintained in Dulbecco's modified Eagle's medium (DMEM) (Life Technologies Co., Gaithersburg, MD, U.S.A.) supplemented with 10% heat-inactivated fetal bovine serum (FBS) (Life Technologies Co.), 100 U/mL of penicillin, and 100 μg/mL of streptomycin in a 5% CO_2/air incubator at 37 °C.

***In Vitro* Cellular Binding Assay** N87 and SUIT2 cells (2×10^5) were seeded in 24-well plates and incubated for 16 h at 37 °C under 5% CO_2. ^{111}In-labeled Tra-AuNRs solution was added to the wells at a concentration of AuNRs at 0.025 mg/mL. For blocking studies (6 h), overdosed trastuzumab (0.20, 0.74, and 1.70 mg for Tra1-, Tra2-, and Tra3-AuNRs, respectively) was mixed with Tra-AuNRs before being added to the wells. Cells were incubated for 1, 3, and 6 h at 37 °C under 5% CO_2 and then washed four times with PBS. Next, the cells were lysed with 1 M of NaOH and incubated at 37 °C for 1 h. The radioactivity taken up by the cells was measured using a γ-counter (2470 WIZARD; PerkinElmer, Inc., Waltham, MA, U.S.A.), followed by the measurement of protein concentration using a Bicinchoninic Acid Protein Assay Kit (Thermo Fisher Scientific Inc., Waltham, MA, U.S.A.). The uptake of ^{111}In-labeled Tra-AuNRs was represented as the percentage dose/mg protein.

Binding Affinity of Tra-AuNRs to HER2 The binding affinities of Tra1-, Tra2-, and Tra3-AuNRs to HER2 were evaluated by calculating the dissociation equilibrium constant (K_d). N87 cells were seeded into six-well plates (1.2×10^6 cells/well) and incubated in a 5% CO_2/air incubator at 37 °C for 16 h. Tra-AuNRs conjugated with different amounts of trastuzumab were dissolved in FBS-free DMEM and added to cells followed by incubation for 6 h at 4 °C. As a blocking group, a mixture of Tra-AuNRs and excess trastuzumab was added to cells. Of note, the AuNRs concentration in Tra-AuNRs ranged from 1 to 200 μg/mL, whereas the concentration of trastuzumab ranged from 5 to 150 μg/mL. After incubation, the medium was removed, and the cells were washed three times with PBS at 4 °C. Cells were collected and counted twice. To lyse the cells, 50 μL of Triton X (1%) and 50 μL of HCl (12 M) were added. The binding of Tra-AuNRs to HER2 was confirmed by measuring the absorbance of AuNRs at 802 nm according to the protocol in our previous report.[24] The results of Tra1-, Tra2-, and Tra3-AuNRs were then compared to determine the most suitable probe.

Animal Models Animal studies were conducted in accordance with the institutional guidelines of Kyoto University, and the experimental procedures were approved by the Kyoto University Animal Care Committee. Five-week-old female BALB/c-*nu*/*nu* nude mice were purchased from Japan SLC (Shizuoka, Japan). The animals were raised in air-conditioned rooms under a 12-h light–dark cycle with free access to food and water. HER2-expressing N87 (2×10^6 cells) and HER2-low-expressing SUIT2 (1×10^6 cells) mixed with Geltrex (Life Technologies Co.) were subcutaneously inoculated into the left and right thighs of the mice, respectively. Biodistribution studies and imaging studies were carried out 2 to 3 weeks after tumor transplantation.

Biodistribution Study *In vivo* biodistribution studies were conducted by using ^{111}In-labeled Tra1-, Tra2-, and Tra3-AuNRs. ^{111}In-Tra-AuNRs (240 μg of AuNRs) with a radiochemical purity of greater than 90% in 200 μL of PBS were intravenously injected into the N87 and SUIT2 tumor-bearing mice. At 48, 72, and 96 h after injection, the organs of interest were excised and weighed; radioactivity counts were determined using a γ-counter (2470 WIZARD) and the injected dose as a standard. Data were calculated as percentage injected dose (%ID)/g tissue. The results of Tra1-, Tra2-, and Tra3-AuNRs were then compared to select the most suitable probe.

***In Vitro* PA Imaging Study** N87 and SUIT2 cells (1×10^6) were seeded in six-well plates and incubated for 16 h at 37 °C under 5% CO_2. Tra1-, Tra2-, and Tra3-AuNRs solutions were added to the wells. For Tra2-AuNRs, overdosed trastuzumab was mixed before the addition to the cells for blocking studies. Cells were incubated for 6 h at 37 °C under 5% CO_2, followed by washing three times with PBS. The cells were then collected in 0.5-mL tubes and centrifuged to be imaged. The PA instruments were set as follows. The tube was suspended in water and custom optical fibers (NA = 0.22, core diameter: 230 μm; Mitsubishi Cable Industries, Tokyo, Japan), and an ultrasound linear array probe (SL15-4, center frequency: 8 MHz; SuperSonic Imagine, Aix-en-Provence, France) was used to take ultrasound images. We used an ultrasound system, Aixplorer (SuperSonic Imagine, Aix-en-Provence, France), as an ultrasound device. PA signal intensity ratios were calculated by dividing PA signals of cells treated with Tra-AuNRs by PA signals of background (water).

SPECT Imaging Study According to the results of the biodistribution and affinity studies, Tra2-AuNRs were considered to be most promising for further *in vivo* imaging examination.

^{111}In-Tra2-AuNRs (7.4 MBq, 200 μL of PBS) were intravenously injected into N87 and SUIT2 tumor-bearing mice. Subsequently, the mice were anesthetized with isoflurane, and SPECT/CT images were obtained by using the U-SPECT-II system (MILabs, Utrecht, the Netherlands) with 1.0-mm pinhole collimators (SPECT conditions: 30 min × 1 frame; CT conditions: accurate full-angle mode in 65 kV/615 μA) at 96 h after injection. SPECT images were reconstructed by using the ordered subset expectation maximization method (8 subsets, 1 iteration) with a 0.8-mm Gaussian filter.

Statistical Analysis Each experiment was individually conducted at least three times. The statistical significance among groups was identified by using two-way ANOVA followed by Tukey's test for *in vitro* cellular uptake study and for biodistribution study and by using Dunnett's test for *in vitro* PA imaging study. Data are expressed as means ± standard

deviations, and p-values less than 0.05 were considered statistically significant.

RESULTS

Characterization of ^{111}In-Tra-AuNRs Series The Tra-AuNRs series prepared in this study were referred to as either Tra1-AuNRs, Tra2-AuNRs, or Tra3-AuNRs, depending on the number of trastuzumab molecules conjugated to AuNRs. More specifically, the numbers of trastuzumab molecules conjugated to AuNRs in Tra1-, Tra2-, or Tra3-AuNRs were 0.6 ± 0.1, 2.3 ± 0.2, and 5.3 ± 0.2, respectively. When DTPA-Tra-AuNRs were reacted with $^{111}InCl_3$, the decay-corrected radiochemical yields at end of synthesis for ^{111}In-Tra1-, ^{111}In-Tra2-, and ^{111}In-Tra3-AuNRs were 8.9, 11.2, and 12.6%, respectively. Additionally, the radiochemical purity of ^{111}In-Tra-AuNRs used in the following experiments was over 90%.

The stability of ^{111}In-Tra-AuNRs as evaluated by using the size-exclusion column method is summarized in Table 1. The purity of each probe was more than 95%, indicating that they remained stable after 96 h of incubation in PBS and mouse serum.

***In Vitro* Cellular Binding Assay** The cellular binding of the Tra-AuNRs series was evaluated by measuring the radioactivity of ^{111}In-labeled Tra-AuNRs taken up by the tumor cells, which is summarized in Fig. 1. When Tra-AuNRs series were added to N87 cells, the radioactivity bound to cells gradually increased over time. Higher binding was observed in Tra2- and Tra3-AuNR-supplemented N87 cells than in Tra1-AuNR-supplemented cells as the number of trastuzumab molecules conjugated to AuNRs increased, and there was no significant difference between the Tra2- and Tra3-AuNRs in this regard. On the other hand, there were no significant changes in radioactivity taken up by SUIT2 cells regardless of whether the amount of trastuzumab bound to AuNRs changed. The radioactivity of ^{111}In-labeled Tra-AuNRs in N87 cells when treated with overdosed trastuzumab decreased to the same level as that observed in SUIT2 cells at 6 h after incubation.

Binding Affinity of the Tra-AuNRs Series to HER2 The K_d values of the Tra-AuNRs series to HER2 was determined by measuring the absorbance of AuNRs taken up by HER2-positive N87 cells. The K_d values of Tra1-, Tra2-, and Tra3-AuNRs were 99.0 ± 54.7, 42.7 ± 15.5, and 37.7 ± 15.5 nM, respectively. The binding affinity of Tra-AuNRs series increased as the number of trastuzumab molecules conjugated to AuNRs increased, though not significantly.

Biodistribution of Tra-AuNRs Series in Tumor-Bearing Mice The results of biodistribution studies of the ^{111}In-Tra-AuNRs series using N87 and SUIT2 tumor-bearing mice are summarized in Table 2 and Fig. 2. Only the accumulation of ^{111}In-Tra2-AuNRs at 96 h after injection presented significant differences in N87 and SUIT2 tumors of 9.41 ± 1.29 and 5.57 ± 1.19%ID/g, respectively (Table 2). The mean tumor-to-blood ratio, which is an indicator of imaging contrast, was 4.18 ± 0.88 for N87 tumors, which was enough to obtain high-contrast images and which was significantly higher than that for SUIT2 tumors (2.43 ± 0.39). All three kinds of ^{111}In-Tra-AuNRs accumulated considerably in the liver and spleen, and the hepatic uptake increased as the number of trastuzumab molecules conjugated to AuNRs increased. The accumulation in the liver decreased gradually after 96 h, whereas the accumulation in the spleen remained longer.

***In Vitro* PA Imaging Study** The cellular uptakes of the Tra-AuNRs series were evaluated by *in vitro* PA imaging using the devices presented in Figs. 3A–C. N87 cells demonstrated stronger PA signals than SUIT2 cells when incubated

Table 1. Radiochemical Purity of ^{111}In-Tra-AuNRs Series after 48, 72, and 96 h Incubation at 37 °C in PBS and Serum

	^{111}In-Tra1-AuNRs		^{111}In-Tra2-AuNRs		^{111}In-Tra3-AuNRs	
	PBS	Serum	PBS	Serum	PBS	Serum
48 h	97.5%	98.3%	99.4%	99.4%	98.3%	99.2%
72 h	96.3%	98.0%	99.3%	99.3%	98.5%	99.2%
96 h	95.8%	98.0%	99.1%	99.1%	97.6%	99.1%

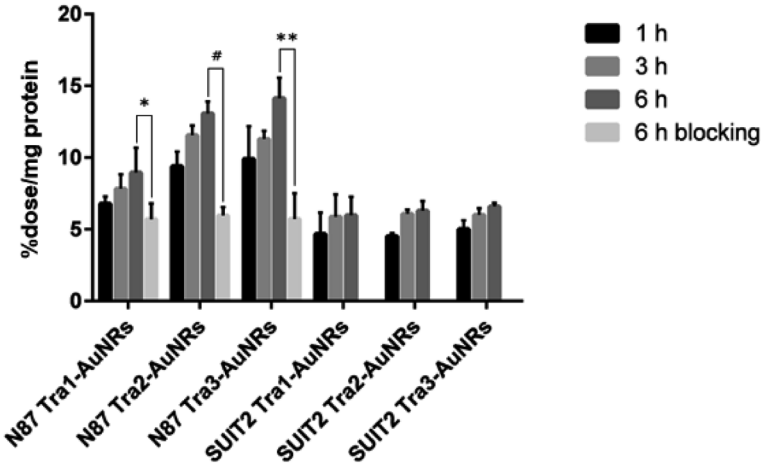

Fig. 1. Cellular Uptake Study Using HER2 Positive and Negative Cells

The cellular binding of Tra1-, Tra2-, and Tra-3-AuNRs to N87 and SUIT2 cells with different incubation times. $^{*}p < 0.05$, $^{**}p < 0.01$, $^{\#}p < 0.001$.

Table 2. Biodistribution of Radioactivity (%ID/g) after the Injection of ^{111}In-Tra-AuNRs Series

	48 h	72 h	96 h
Time after the injection of ^{111}In-Tra1-AuNRs			
Blood	9.06 ± 4.06	5.10 ± 2.44	3.48 ± 1.08
Heart	0.83 ± 1.44	0.35 ± 0.45	1.18 ± 1.04
Lungs	3.59 ± 0.50	1.46 ± 0.97	1.58 ± 0.17
Liver	24.79 ± 2.39	23.26 ± 2.51	16.97 ± 1.61
Kidney	7.13 ± 0.50	6.76 ± 1.71	4.66 ± 0.54
Stomach	0.61 ± 0.44	0.16 ± 0.18	0.19 ± 0.25
Intestine	0.98 ± 0.29	0.60 ± 0.08	0.69 ± 0.15
Pancreas	1.40 ± 0.95	0.54 ± 0.63	1.04 ± 1.15
Spleen	23.87 ± 6.03	20.14 ± 6.92	14.31 ± 3.72
Muscle	0.34 ± 0.56	0.64 ± 0.78	1.34 ± 1.49
N87	14.80 ± 4.01	14.80 ± 7.96	16.91 ± 5.78
SUIT2	11.72 ± 4.10	13.48 ± 8.01	12.26 ± 2.65
Time after the injection of ^{111}In-Tra2-AuNRs			
Blood	4.32 ± 0.55	3.80 ± 0.84	2.28 ± 0.23
Heart	0.68 ± 0.22	0.95 ± 0.40	0.27 ± 0.27
Lungs	1.92 ± 0.43	1.88 ± 0.61	1.09 ± 0.05
Liver	34.20 ± 1.66	33.18 ± 1.91	26.85 ± 1.06
Kidney	8.30 ± 0.86	7.78 ± 0.82	4.76 ± 0.36
Stomach	0.49 ± 0.05	0.34 ± 0.24	0.24 ± 0.05
Intestine	0.69 ± 0.02	0.57 ± 0.11	0.38 ± 0.02
Pancreas	0.57 ± 0.13	0.50 ± 0.08	0.33 ± 0.12
Spleen	14.50 ± 5.32	14.74 ± 1.75	11.55 ± 0.86
Muscle	0.38 ± 0.20	0.61 ± 0.07	0.25 ± 0.20
N87	9.35 ± 1.47	10.80 ± 1.45	9.41 ± 1.29*
SUIT2	7.44 ± 0.88	8.00 ± 0.97	5.57 ± 1.19
Time after the injection of ^{111}In-Tra3-AuNRs			
Blood	3.55 ± 0.08	2.51 ± 0.97	1.77 ± 0.80
Heart	1.10 ± 0.38	0.97 ± 0.25	0.73 ± 0.39
Lungs	1.83 ± 0.08	1.47 ± 0.22	0.94 ± 0.58
Liver	39.86 ± 6.71	34.71 ± 7.80	30.31 ± 10.75
Kidney	6.79 ± 0.95	5.17 ± 0.71	4.40 ± 0.94
Stomach	0.30 ± 0.15	0.50 ± 0.10	0.41 ± 0.33
Intestine	0.66 ± 0.09	0.60 ± 0.07	0.61 ± 0.19
Pancreas	0.60 ± 0.42	0.42 ± 0.12	0.57 ± 0.45
Spleen	28.06 ± 1.12	27.07 ± 7.77	21.20 ± 7.58
Muscle	0.78 ± 0.90	0.65 ± 0.74	0.81 ± 0.36
N87	5.86 ± 0.57	6.67 ± 1.67	4.39 ± 0.35
SUIT2	5.26 ± 0.47	4.38 ± 1.36	4.13 ± 1.99

Each value represents the mean ± standard deviation ($n = 3$). *$p < 0.05$ *vs.* SUIT2.

with Tra-AuNRs series for 6 h (Fig. 3D). The PA signals in N87 cells were 4.7-fold higher than those in SUIT2 cells when treated with Tra2-AuNRs (Fig. 3E). Furthermore, N87 cells incubated with Tra2- and Tra3-AuNRs demonstrated stronger signals than those incubated with Tra1-AuNRs, indicating more AuNRs bound as a result of more trastuzumab conjugation. The PA signal in N87 was significantly decreased by 20% when the cells were co-treated with overdosed trastuzumab, suggesting HER2-specific binding of Tra2-AuNRs (Figs. 3D, E). PA signals were partially observed in SUIT2 cells probably due to non-specific nanoparticle uptake.

SPECT Imaging Considering the results of both biodistribution studies and *in vitro* binding affinity of the Tra-AuNRs series to HER2, Tra2-AuNRs were chosen for the following imaging study.

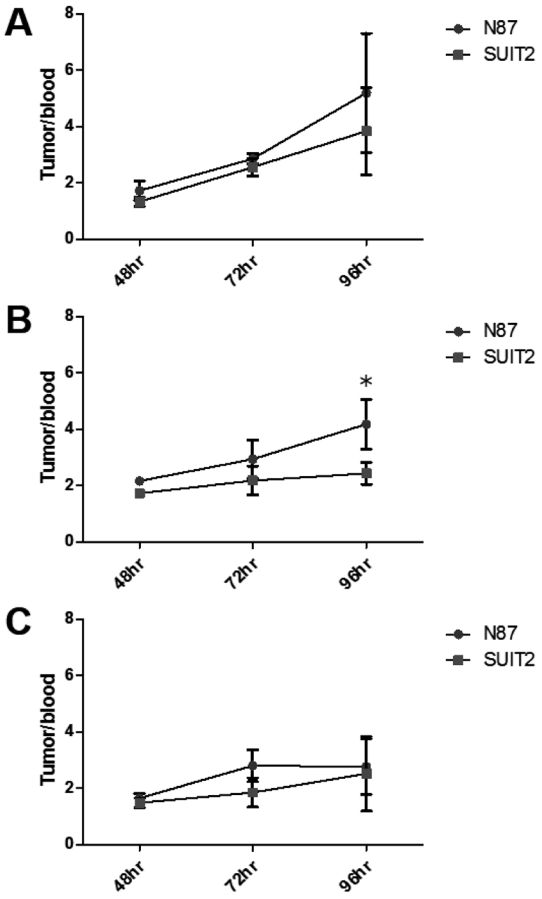

Fig. 2. Tumor-to-Blood Ratios Using HER2 Positive and Negative Dual Tumor Bearing Mice

Tumor-to-blood ratios following the injection of ^{111}In-Tra-AuNRs series (mean ± standard deviation, $n = 3$). A: ^{111}In-Tra1-AuNRs. B: ^{111}In-Tra2-AuNRs. C: ^{111}In-Tra3-AuNRs. *$p < 0.05$.

SPECT images of tumor-bearing mice at 96 h after administration with ^{111}In-Tra2-AuNRs are presented in Fig. 4. When compared with SUIT2 tumors in the right thighs, the N87 tumors inoculated in the left thighs were clearly visualized, with high background ratios.

DISCUSSION

In this research, ^{111}In-labeled Tra-AuNRs (^{111}In-Tra-AuNRs) series with different amounts of trastuzumab conjugated per AuNRs were prepared and evaluated by both PA imaging and SPECT imaging. The optimized Tra2-AuNRs led to HER2-specific *in vitro* PA imaging and *in vivo* SPECT imaging results, representing the probability of both pre- and intraoperative use.

In the cell-binding assay, more Tra2- and Tra3-AuNRs than Tra1-AuNRs bonded to N87 cells at each time point, whereas the binding counts were similar between Tra2- and Tra3-AuNRs. These outcomes agreed with both affinity results and PA imaging results, indicating that both Tra2- and Tra3-AuNRs were superior to Tra1-AuNRs *in vitro*. The binding counts of all Tra-AuNRs in SUIT2 were significantly less than those in N87 cells, although a partial non-specific binding was

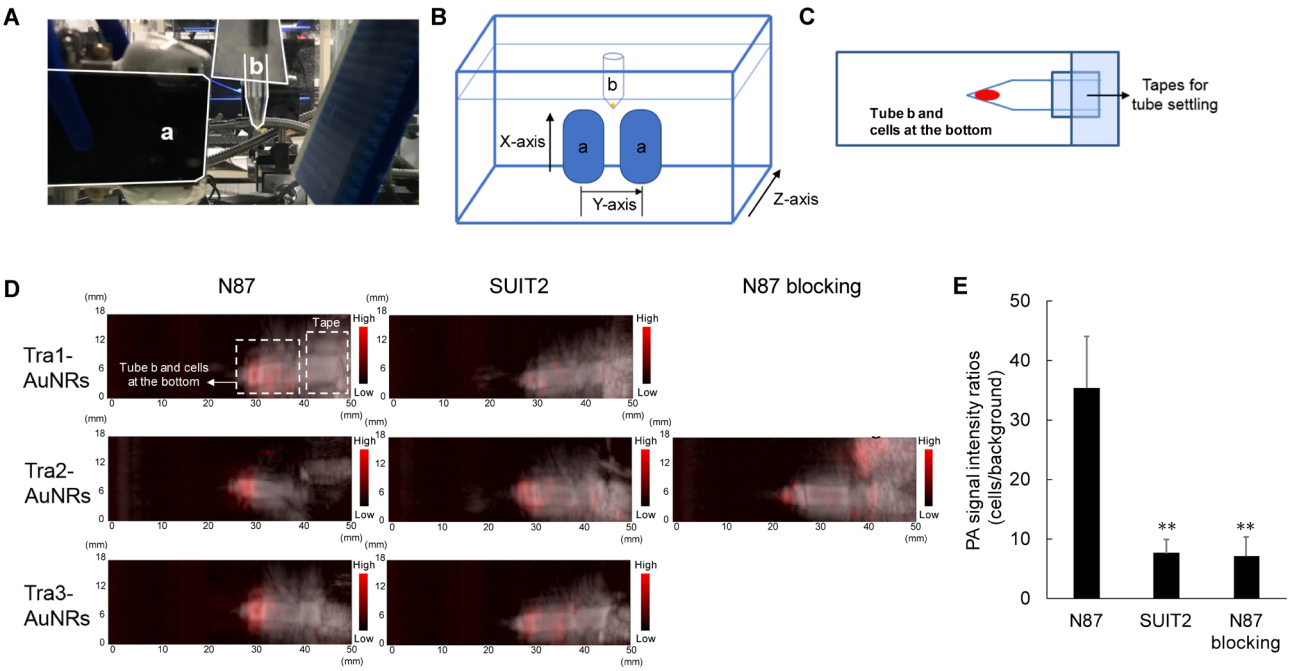

Fig. 3. Photoacoustic Equipment and PA Signals after Tra-AuNRs Incubation with HER2 Positive and Negative Cells

A: PA measuring instruments used for *in vitro* PA imaging. (a) Light illuminator and ultrasound-wave receiver. (b) A sample tube with cells at its bottom was hung over the water tank. B: Diagram of the PA imaging instrument. Sample tube with cells (b) at its bottom was hung and sensor (a) moved in a range of 18 mm to take signals from the sample. The *X*-axis and *Y*-axis were corresponded to ones in each pictures in Fig. 3D. C: Diagram of the PA images. The cells were collected to the bottom of the tube as shown. Then, the tube was sunk into the water. D: *In vitro* PA imaging study of Tra1-, Tra2-, and Tra3-AuNRs using both N87 and SUIT2 cells after 6 h of incubation. E. PA signal intensity ratios of Tra2-AuNRs-added cell samples, calculated by dividing PA signals of cells by PA signals of background. $^{**}p < 0.01$. (Color figure can be accessed in the online version.)

observed. The addition of overdosed trastuzumab reduced the binding in N87 cells indicated the HER2-specific binding of Tra-AuNRs. The reduced binding of Tra1-AuNRs is probably because of the much fewer trastuzumab molecules conjugated.

In biodistribution studies, at each time point, as the number of trastuzumab molecules conjugated to AuNRs increased, the accumulation in both N87 and SUIT2 tumors decreased, and faster blood clearance and higher accumulation in the liver and spleen were also observed. For instance, at 48 h after probe injection, 9.06%ID/g of Tra1-AuNRs remained in the blood, whereas 3.55%ID/g of Tra3-AuNRs remained. Meanwhile, in the liver at the same time point, 24.79%ID/g of Tra1-AuNRs remained, whereas 39.86%ID/g of Tra3-AuNRs remained. High uptakes of probes by the reticuloendothelial system (RES) led to lower tumor accumulations. More trastuzumab molecules conjugated to the surface of AuNRs resulted in less surface area covered with polyethylene glycol (PEG), and it has been widely reported that the introduction of antibodies to the surface of nanoparticles accompanied by less surface area of PEG leads to higher accumulations in the RES.[25,26] However, the tumor uptake of ^{111}In-Tra2-AuNRs (9.41%ID/g at 96 h post-injection) was much higher than that of gold nanoparticles (1.23%ID/g at 48 h in MDA-MB-361 tumor),[22] which was well consistent with the previous data that the tumor accumulation of AuNRs is superior to that of gold nanoparticles.[23] Jokerst *et al.* reported a PA imaging of ovarian cancer using AuNRs.[27] Even if the tumor uptake of AuNRs was about 2–3%ID/g, ovarian cancer was detected by PA imaging; therefore, we expected that Tra2-AuNRs could sensitively detect HER2-positive tumors by PA imaging. On the other hand, a partial non-specific accumulation of Tra-AuNRs in HER2-negative tumors was observed. In order

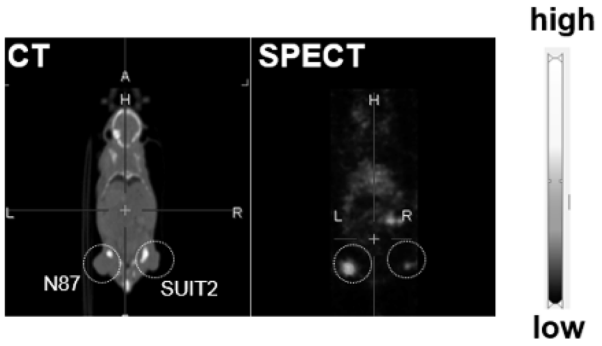

Fig. 4. SPECT Result after Administration of ^{111}In-Tra2-AuNRs

Coronal SPECT/CT images of Balb/c nude mouse inoculated with N87 (HER2-positive, left thigh) and SUIT2 (HER2-negative, right thigh) at 96 h after ^{111}In-Tra2-AuNR administration.

to achieve a precise diagnosis of HER2-positive tumors, the specificity of Tra-AuNRs to HER2 needs to be improved in the future. Furthermore, the marked uptake of Tra-AuNRs by RES (liver and spleen) would limit the use of Tra-AuNRs for abdominal cancer. However, due to the lower uptake of Tra-AuNRs in the chest organs, Tra-AuNRs would have a potential for HER2-positive breast tumor imaging. The tumor-to-blood ratios were approximately 4 for ^{111}In-Tra2-AuNRs, suggesting the possibility of high contrast tumor imaging.

In a previous study using ^{111}In-trastuzumab for imaging HER2-positive tumors (N87),[28] the tumor accumulation of ^{111}In-trastuzumab was approximately 15%ID/g at 48 h post-injection, which was about 1.5-fold higher than that of ^{111}In-Tra2-AuNRs. On the other hand, ^{111}In-Tra2-AuNRs showed the higher non-specific accumulation in the liver and the lower ones in the spleen and kidney than ^{111}In-trastuzumab. The

tumor-to-blood ratios of ^{111}In-Tra2-AuNRs were equal to or higher than those of ^{111}In-trastuzumab, indicating the high-contrast tumor imaging by ^{111}In-Tra2-AuNRs.

Furthermore, there might be more applications of radiolabeled trastuzumab-AuNRs. ^{111}In can be replaced by yttrium-90 (^{90}Y, β^--ray-emitting radiometal, 2.28 MeV, $t_{1/2} = 64.0$ h), which is widely used for cancer-targeted radiotherapy. By optimizing the level of accumulation in the tumor, liver, and spleen, it is likely possible to use ^{90}Y-labeled Tra-AuNRs as a cancer treatment agent. Furthermore, with the excellent photothermal effect of AuNRs,[29,30] more effective treatment and less side effects could be achieved by irradiating the AuNR-accumulated tumors with NIR light at the appropriate wavelength. Of note, cancer cells around AuNRs could be damaged after the temperature of AuNRs reaches 42 °C.

CONCLUSION

In this study, we developed a series of ^{111}In-labeled Tra-AuNRs, and ^{111}In-Tra2-AuNRs demonstrated high affinity toward HER2 and an excellent biodistribution profile. Furthermore, ^{111}In-Tra2-AuNRs revealed HER2-specific binding to HER2-expressing tumor cells and enabled HER2-specific PA imaging *in vitro*. Tra2-AuNRs also presented HER2-specific SPECT imaging *in vivo*. These results suggest that Tra2-AuNRs would serve as a robust SPECT and PA dual-imaging probe for the pre- and intraoperative diagnosis of malignant tumors.

Acknowledgments This research was supported by the JSPS KAKENHI program, under Grant Numbers 15H04637 (H. S.) and 16K15316 (K. S.) and by Grant-in-Aid for JSPS Research Fellows (N. D.).

Conflict of Interest The authors declare no conflict of interest.

REFERENCES

1) Bray F, Ferlay J, Soerjomataram I, Siegel RL, Torre LA, Jemal A. Global cancer statistics 2018: GLOBOCAN estimates of incidence and mortality worldwide for 36 cancers in 185 countries. *CA Cancer J. Clin.*, **68**, 394–424 (2018).
2) Aliperti LA, Predina JD, Vachani A, Singhal S. Local and systemic recurrence is the Achilles heel of cancer surgery. *Ann. Surg. Oncol.*, **18**, 603–607 (2011).
3) Jiang JX, Keating JJ, Jesus EM, Judy RP, Madajewski B, Venegas O, Okusanya OT, Singhal S. Optimization of the enhanced permeability and retention effect for near-infrared imaging of solid tumors with indocyanine green. *Am. J. Nucl. Med. Mol. Imaging*, **5**, 390–400 (2015).
4) Tanaka T, Terai Y, Ono YJ, Fujiwara S, Tanaka Y, Sasaki H, Tsunetoh S, Kanemura M, Yamamoto K, Yamada T, Ohmichi M. Preoperative MRI and intraoperative frozen section diagnosis of myometrial invasion in patients with endometrial cancer. *Int. J. Gynecol. Cancer*, **25**, 879–883 (2015).
5) Arita J, Ono Y, Takahashi M, Inoue Y, Takahashi Y, Matsueda K, Saiura A. Routine preoperative liver-specific magnetic resonance imaging does not exclude the necessity of contrast-enhanced intraoperative ultrasound in hepatic resection for colorectal liver metastasis. *Ann. Surg.*, **262**, 1086–1091 (2015).
6) Xiao Q, Chen T, Chen S. Fluorescent contrast agents for tumor surgery. *Exp. Ther. Med.*, **16**, 1577–1585 (2018).
7) Nie J, Zhang J, Gao J, Guo L, Zhou H, Hu Y, Zhu C, Li Q, Ma X. Diagnostic role of ^{18}F-FDG PET/MRI in patients with gynecological malignancies of the pelvis: a systematic review and meta-analysis. *PLOS ONE*, **12**, e0175401 (2017).
8) Zhu D, Wang L, Zhang H, Chen J, Wang Y, Byanju S, Liao M. Prognostic value of ^{18}F-FDG-PET/CT parameters in patients with pancreatic carcinoma: a systematic review and meta-analysis. *Medicine*, **96**, e7813 (2017).
9) Nomori H, Cong Y, Sugimura H. Utility and pitfalls of sentinel node identification using indocyanine green during segmentectomy for cT1N0M0 non-small cell lung cancer. *Surg. Today*, **46**, 908–913 (2016).
10) Kim HK, Quan YH, Choi BH, Park JH, Han KN, Choi Y, Kim BM, Choi YH. Intraoperative pulmonary neoplasm identification using near-infrared fluorescence imaging. *Eur. J. Cardiothorac. Surg.*, **49**, 1497–1502 (2016).
11) Tam AC. Applications of photoacoustic sensing techniques. *Rev. Mod. Phys.*, **58**, 381–431 (1986).
12) Tsujita K. Toward the medical application of photoacoustic Imaging-Fusion of ultrasound imaging and photoacoustic imaging. *Nippon Laser Igakkaishi*, **33**, 380–385 (2013).
13) Kanazaki K, Sano K, Makino A, Yamauchi F, Takahashi A, Homma T, Ono M, Saji H. Feasibility of poly(ethylene glycol) derivatives as diagnostic drug carriers for tumor imaging. *J. Control. Release*, **226**, 115–123 (2016).
14) Kanazaki K, Sano K, Makino A, Homma T, Ono M, Saji H. Poly-oxazoline multivalently conjugated with indocyanine green for sensitive *in vivo* photoacoustic imaging of tumors. *Sci. Rep.*, **6**, 33798–33807 (2016).
15) Sano K, Ohashi M, Kanazaki K, Makino A, Ding N, Deguchi J, Kanada Y, Ono M, Saji H. Indocyanine green-labeled polysarcosine for *in vivo* photoacoustic tumor imaging. *Bioconjug. Chem.*, **28**, 1024–1030 (2017).
16) Cheng K, Kothapalli SR, Liu H, Koh AL, Jokerst JV, Jiang H, Yang M, Li J, Levi J, Wu JC, Gambhir SS, Cheng Z. Construction and validation of nano gold tripods for molecular imaging of living subjects. *J. Am. Chem. Soc.*, **136**, 3560–3571 (2014).
17) Chen YS, Zhao Y, Yoon SJ, Gambhir SS, Emelianov S. Miniature gold nanorods for photoacoustic molecular imaging in the second near-infrared optical window. *Nat. Nanotechnol.*, **14**, 465–472 (2019).
18) Kanazaki K, Sano K, Makino A, Takahashi A, Deguchi J, Ohashi M, Temma T, Ono M, Saji H. Development of human serum albumin conjugated with near-infrared dye for photoacoustic tumor imaging. *J. Biomed. Opt.*, **19**, 096002 (2014).
19) An L, Wang Y, Tian Q, Yang S. Small gold nanorods: Recent advances in synthesis, biological imaging, and cancer therapy. *Materials*, **10**, 1372–1392 (2017).
20) Zhong J, Wen L, Yang S, Xiang L, Chen Q, Xing D. Imaging-guided high-efficient photoacoustic tumor therapy with targeting gold nanorods. *Nanomedicine*, **11**, 1499–1509 (2015).
21) Slamon DJ, Godolphin W, Jones LA, Holt JA, Wong SG, Keith DE, Levin WJ, Stuart SG, Udove J, Ullrich A, Press MF. Studies of the HER-2/neu proto-oncogene in human breast and ovarian cancer. *Science*, **244**, 707–712 (1989).
22) Chattopadhyay N, Fonge H, Cai Z, Scollard D, Lechtman E, Done SJ, Pignol JP, Reilly RM. Role of antibody-mediated tumor targeting and route of administration in nanoparticle tumor accumulation *in vivo*. *Mol. Pharm.*, **9**, 2168–2179 (2012).
23) Puvanakrishnan P, Park J, Chatterjee D, Krishnan S, Tunnell JW. *In vivo* tumor targeting of gold nanoparticles: effect of particle type and dosing strategy. *Int. J. Nanomedicine*, **7**, 1251–1258 (2012).
24) Ding N, Sano K, Kanazaki K, Ohashi M, Deguchi J, Kanada Y, Ono M, Saji H. *In vivo* HER2-targeted magnetic resonance tumor imaging using iron oxide nanoparticles conjugated with anti-HER2 fragment antibody. *Mol. Imaging Biol.*, **18**, 870–876 (2016).

25) Mamot C, Ritschard R, Wicki A, Stehle G, Dieterle T, Bubendorf L, Hilker C, Deuster S, Herrmann R, Rochlitz C. Tolerability, safety, pharmacokinetics, and efficacy of doxorubicin-loaded anti-EGFR immunoliposomes in advanced solid tumours: a phase 1 dose-escalation study. *Lancet Oncol.*, **13**, 1234–1241 (2012).
26) Kennedy LC, Bickford LR, Lewinski NA, Coughlin AJ, Hu Y, Day ES, West JL, Drezek RA. A new era for cancer treatment: Gold-nanoparticle-mediated thermal therapies. *Small*, **7**, 169–183 (2011).
27) Jokerst JV, Cole AJ, Van de Sompel D, Gambhir SS. Gold nanorods for ovarian cancer detection with photoacoustic imaging and resection guidance *via* Raman imaging in living mice. *ACS Nano*, **6**, 10366–10377 (2012).
28) Kuo WY, Lin JJ, Hsu HJ, Chen HS, Yang AS, Wu CY. Noninvasive assessment of characteristics of novel anti-HER2 antibodies by molecular imaging in a human gastric cancer xenograft-bearing mouse model. *Sci. Rep.*, **8**, 13735 (2018).
29) Ratto F, Matteini P, Centi S, Rossi F, Pini R. Gold nanorods as new nanochromophores for photothermal therapies. *J. Biophotonics*, **4**, 64–73 (2011).
30) Choi WI, Sahu A, Kim YH, Tae G. Photothermal cancer therapy and imaging based on gold nanorods. *Ann. Biomed. Eng.*, **40**, 534–546 (2012).